Review guidelines

Please in full read before you begin

How to review

When ready **submit your review online**. The review form is divided into 5 sections. Please consider these when composing your review:

1. **BASIC REPORTING**
2. **EXPERIMENTAL DESIGN**
3. **VALIDITY OF THE FINDINGS**
4. General comments
5. Confidential notes to the editor

You can also annotate this **pdf** and upload it as part of your review

To finish, enter your editorial recommendation (accept, revise or reject) and submit.

BASIC REPORTING

- Clear, unambiguous, professional English language used throughout.
- Intro & background to show context. Literature well referenced & relevant.
- Structure conforms to **PeerJ standard**, discipline norm, or improved for clarity.
- Figures are relevant, high quality, well labelled & described.
- Raw data supplied (See **PeerJ policy**).

EXPERIMENTAL DESIGN

- Original primary research within **Scope of the journal**.
- Research question well defined, relevant & meaningful. It is stated how research fills an identified knowledge gap.
- Rigorous investigation performed to a high technical & ethical standard.
- Methods described with sufficient detail & information to replicate.

VALIDITY OF THE FINDINGS

- Impact and novelty not assessed. Negative/inconclusive results accepted. *Meaningful* replication encouraged where rationale & benefit to literature is clearly stated.
- Data is robust, statistically sound, & controlled.
- Conclusion well stated, linked to original research question & limited to supporting results.
- Speculation is welcome, but should be identified as such.

The above is the editorial criteria summary. To view in full visit **https://peerj.com/about/editorial-criteria/**

Cranial bone histology of *Metoposaurus krasiejowensis* (Amphibia, Temnospondyli) from the Late Triassic of Poland

Kamil Gruntmejer[1,2,*], Dorota Konietzko-Meier[1,2,3], Adam Bodzioch[1]

[1] Opole University, Department of Biosystematics, Laboratory of Palaeobiology, Oleska 22, 45-052 Opole, Poland

[2] Opole University, European Centre of Palaeontology, Oleska 48, 45-052 Opole, Poland

[3] University of Bonn, Steinmann Institute, Nussallee 8, 53115 Bonn, Germany

[*]gruntmejerkamil@gmail.com

* - corresponding author

ABSTRACT

In this study a detailed description of the 21 skull bones of *Metoposaurus krasiejowensis* from the Late Triassic of Poland is presented. All dermal bones show a diploë structure, with the ornamented external surface. The ridges consist of well vascularized parallel-fibered bone; the valleys are built of an avascular layer of lamellar bone. The dense clumps of thin, well mineralized Sharpey's fibers are preserved. The growth marks are manifested in four ways: a sequence of resting lines; layers of lamellar bone alternated with layers with Interwoven Structural Fibers (ISF); thick, avascular annuli and high vascularized zones; and the alternations of valleys and ridges. The thick middle region consists of cancellous bone, with varying porosity. The thin and less vascularized internal cortex consists of parallel-fibered bone. Calcified cartilage is observed in the quadrate and the exoccipital. The skull bones show strong variability within the microanatomical and histological levels. The histological framework is not bone-limited, but varies even in one single bone; this seems to be related to the specific position of the bone and depends on the local biomechanical loading of the particular part of the skull. The large accumulation of Sharpey's fibers in the occipital condyles indicates the presence of strong muscles and ligaments connecting the skull to the vertebral column. The dynamic processes during the ornamentation deposition are observed indicate that the position of the ridges and grooves change during the growth and could be the specific adaptation to biomechanical conditions and stress distribution during the bone development. In the supratemporal the

cementing lines indicated the remodeling process could be involved into the creations of sculpture.

Keywords:
dermal bones, skull, microanatomy, growth pattern

INTRODUCTION

Metoposaurids were large, up to 3 meters long, late Triassic Temnospondyli with a strongly dorso-ventrally flattened body, and well adapted to aquatic life. The most characteristic and best known part of the *Metoposaurus* skeleton is the extremely flat parabolic skull with anteriorly located orbits (*e.g*. Schoch & Milner, 2000).

The flat bones of the skull develop via direct transformation of preexisting connective tissue (Francillion-Vieillot et al., 1990). The external surface of the dermal bones is characteristically ornamented. A network of raised, reticulate ridges that enclose approximately flat-bottomed, interlocking, polygonal cells is the most common type. The vast majority of these cells are four-, five-, or six-sided, creating a honeycomb- or waffle iron-like texture. In some temnospondyls, this is essentially the only texture present. The second texture type comprises raised, parallel to sub-parallel ridges separated by round-bottomed grooves (Rinehart & Lucas, 2013). The function of the ornamentation is still unclear. The best supported hypotheses suggest the increase the surface area for skin supports, increasing the strength of the bone or the protection of blood vessels (summarized in Coldiron, 1974; Witzmann, 2009; Rinehart & Lucas, 2013).

The histology of temnospondyl dermal bones was first described by Gross (1934), who provided a short description of the skull bones of *Mastodonsaurus*, *Metoposaurus* and *Plagiosternum*, and recognized that the dermal bones exhibit a diploë structure. Later, histological studies on the dermal bones in Temnospondyli have focused mainly on morphology, vascular network and collagen fibres organization (Bystrow, 1947; Enlow & Brown, 1956; Coldiron, 1974; de Ricqlès, 1981; Castanet *et al*, 2003; Scheyer, 2007) and were limited only to the few taxa. The systematic studies of dermal bones within numerous tetrapod taxa were provided by Witzmann (2009) and de Buffrénil et al. (2016).

Recent the histological studies of metoposaurids have focused mainly on the long bones, ribs and vertebrae (Steyer et al., 2004; Gądek, 2012; Konietzko-Meier & Klein, 2013; Konietzko-Meier & Sander, 2013; Konietzko-Meier et al., 2013; Koniezko-Meier et al., 2014). Up until now the dermal bones of *Metoposaurus* have not been studied in detail histologically. The only record of the histological description of *Metoposaurus diagnosticus* dermal bone was given by Gross (1934) and later re-described by Witzmann (2009). However, it is unclear if the illustrated section was derived from the skull or the pectoral girdle, or even if the tested bone-fragment belongs to *Metoposaurus* at all.

The main goal of this study is to present the detailed description of the histology of almost all bones from one skull and determine, if possible, the tendencies and variability of the histological framework from the one *Metoposaurus krasiejowensis* (Sulej, 2002) skull. The temnospondyl skull functionally represents one skeletal element, however, anatomically, it is a conglomerate of numerous bones various in shape and thickness, having various functions and biomechanical loading (i.e. Fortuny et al., 2011, Fortuny et al., 2012). Another question that arises is if the various functions of the single bones are also reflected in the histology, and if the

histological data may be useful for interpretations the skull mechanics. The results of this question, however, will be published as a separate paper.

MATERIAL AND METHODS

Material – The skull (UOPB 01029; 40 cm in length) of *Metoposaurus krasiejowensis* was studied histologically (Figs. 1 and 2). The roof side of the skull was almost completely preserved, whereas on the palatal side only the fragments of the vomer, parasphenoid, pterygoids, quadrates and exoccipitals were preserved. The species discovered in Poland was originally described as *Metoposaurus diagnosticus krasiejowensis* Sulej, 2002, the subspecies of an older *Metoposaurus diagnosticus* (Meyer, 1842). Brusatte *et al*. (2015) resigned using the subspecies for the German *M. diagnosticus diagnosticus* (von Meyer, 1842) and the Polish *M. diagnosticus krasiejowensis* and suggested to refer both taxa on the separate species level as *M. diagnosticus* and *M. krasiejowensis* instead. This taxonomy is followed in this study.

Locality – The examined material comes from the famous locality in Krasiejów where a large number of disarticulated skeletons have been discovered in the Upper Triassic (Keuper), fine-grained, continental sediments. The bones can be found in two main bone-bearing horizons referred to as the lower and the upper horizon (Dzik & Sulej, 2007). The lower horizon has been deposited on an alluvial plain during a catastrophic mud-flow event (Bodzioch & Kowal-Linka, 2012). The skull presented here, has been excavated from the less than 1 m thick lower bone-bearing layer, which is very rich in *Metoposaurus krasiejowensis* remains accompanied by relatively a high diversified fossil assemblage. Vertebrates are represented by a second temnospondyl, *Cyclotosaurus intermedius* (Sulej & Majer, 2005), a phytosaur (*Palaeorhinus*; see Dzik, 2001), a typical terrestrial tetrapod aetosaur *Stagonolepis olenkae* (Sulej, 2010), pterosaurs

(Dzik & Sulej, 2007), until recently undefined till now sphaenodonts and other small tetrapods (Dzik & Sulej, 2007), and fishes (dipnoans described recently by Skrzycki 2014, as well as various actinopterygian and chondrichthyan species). Invertebrates, such as unionid bivalves (Dzik et al., 2000; Dzik & Skawina, 2011; Skawina 2013), cycloids (Dzik, 2008) spinicaudatan crustaceans (Olempska, 2004), fresh-water ostracods (Olempska, 2004, 2011) and some gastropods, are also very common. The upper horizon is restricted to lenses cemented with calcium carbonate, interpreted as a meander deposit (e.g. Gruszka and Zieliński, 2009). It is dominated by strictly terrestrial animals including *Stagonolepis* and the primitive dinosauromorph *Silesaurus opolensis* (Dzik, 2003). Aquatic vertebrates such as amphibians and phytosaurs are less common compared to the lower horizon. Apart from that, one fragmentary specimen of the rauisuchian *Polonosuchus silesiacus* (Brusatte et al., 2010) was excavated between the upper and lower horizons.

According to complex stratigraphic studies of the Upper Silesian Keuper, the bone-bearing beds have been deposited in the early Norian times (Racki & Szulc, 2014; Szulc et al., 2015a, b), however, biochronological speculations uphold the Late Carnian age (e.g. Dzik & Sulej 2007; Lucas et al. 2007; Lucas, 2015).

Methods – The skull was sectioned in 20 planes (Fig. 2) and the thin sections were prepared according to standard petrographic procedures (Lamm, 2014). The thin sections were ground and polished to a thickness of about 60-80 μm using wet SiC grinding powders (SiC 600, 800). Subsequently, the thin sections were studied under a LEICA DMLP light microscope in plane and cross polarized light.

The histological nomenclature follows Francillion-Vieillot et al. (1990) and Witzmann (2009). According to Francillion-Vieillot et al. (1990) the annual growth cycle consists of a

thick, fast growing zone, a thin, slow growing annulus, and a Line of Arrested Growth (LAG). In this study, the term zone is used as in its traditional meaning, for the highly vascularized layer, with lower organization of collagen fibers. The term annulus refers to the layer without vascular canals and higher organization of collagen fibers, but usually similar in thickness as a zone. In the studied material, no clear LAGs can be observed, instead adjacent to the annuli, numerous lines are present. To avoid nomenclature problems, all lines representing the cessation of growth are referred in this study as resting lines, without determination if they occur annually or not (Konietzko-Meier & Sander, 2013) – also see discussion.

In the thin sections, the average thickness of the entire bone and of each layer was estimated, expressed as an arithmetical average from three measurements of the thickness of the entire bone/layer. The thickness of the external layer was measured three times on the distance between the border line with middle region and the bottom of valleys and three times as the distance between the border line with middle region and the top of ridges. The mathematical average was calculated from these measurements. The minimum and maximum thicknesses represent the lowest and largest measurement, respectively, for each described layer. As the borders between external cortex/middle region/internal cortex were taken the line where the clearly visible increasing of the remodeling degree of the middle region is visible (the number of the erosion cavities, independent of their size, is visible higher). For the estimation of the ratio between the three components (E – external cortex, M – middle region, I – internal cortex; E:M:I), the average thickness of the external cortex was taken as one and then proportionally the value for middle region and internal cortex were calculated. Note that the internal cortex of dermal bone is oriented to the visceral surface of the body, thus in parasphenoid, pterygoid and vomer the external cortex is then oriented ventrally.

160 A detailed description of each bone is presented in the Supplementary Material.

161

162 **RESULTS**

163

164 **Microanatomy of dermal bones**

165 Most dermal bones of the skull are flat plates. Only the premaxillas and maxillas possess
166 a more complicated shape (Fig. 3). The premaxilla is built up of three branches: the dental shelf,
167 the alary process (Schoch, 1999) which connects the skull roof to its margin, and the vomeral
168 process, which connects the dental shelf to the vomer (Fig. 3A). The maxilla is built up from two
169 branches, the dorsal branch with an ornamented external cortex, and the ventral branch with the
170 dental shelf (Fig. 3B).

171 The dermal bones show the clear diploë structure (Fig. 4). The external cortex of the
172 skull-roof bones created variably ornamentations build from a combination of grooves or
173 tubercles and ridges (Table 1, Fig. 1), respectively visible in the cross-section as valleys and
174 ridges (Fig. 4A). The thickness of the flat bones varies from under 0.2 to over 10 millimeters
175 (Table 1), with different proportions between the particular layers. No relation can be observed
176 between the thickness of the external cortex and the thickness of the entire bone, i.e. the external
177 cortex of the tabular and postorbital/jugal about one mm thick, and the average thickness of the
178 skull bones is, respectively, almost ten and six mm (Table 1). The relatively thin squamosum 2
179 with an average thickness of only about three mm, developed an external cortex which takes up
180 almost half of the bone thickness (Table 1). The largest part of the bone almost always consists
181 of the middle region (which is two to eleven times thicker as the external cortex), with the
182 exception of squamosum 2, where the middle region is the thinnest (Table 1). The internal cortex

183 is the thinnest of the three layers and composes usually only 20% to 80% of the thickness of
184 external cortex, with the exception of the parasphenoid (Table 1).
185
186 **General histology of dermal bones**
187 **External cortex** – In all sections the external cortex is consists of parallel-fibred bone,
188 whereas in the valleys lamellar bone often occurs (Fig. 4B and C). The elongated osteocyte
189 lacunae with branched canaliculi in the bone matrix are numerous (Fig. 5A). Vascular canals are
190 mostly longitudinally oriented (Fig. 5A, B). The degree of vascularization varies from relatively
191 low in the premaxilla and frontal, moderate in the maxilla and prefrontal, to highly vascularized
192 in the jugal, postorbital, parietal, squamosum, quadratojugal, vomer and parasphenoid. In the
193 nasal, postparietal, postfrontal, tabular and supratemporal, numerous vascular canals within the
194 ridges are visible, which are arranged in rows parallel to the bony surface, whereas the valleys
195 are avascular. The external cortex is dominated by simple vascular canals and primary osteons.
196 In some bones (nasal, lacrimal, prefrontal, tabular, squamosum, vomer and parasphenoid), the
197 secondary osteons and single erosion cavities are visible in the transition region to the middle
198 layer (for details see the Supplementary Material).
199 Typical for the external cortex are distinct collagen fibers (Fig. 5C, E). In some bones (jugal,
200 postorbital, postfronat, postparietal, tabular) they create a thick Intervowen Structural Fibres
201 (ISF) (Fig. 5E). In the premaxilla, maxilla, nasal, lacrimal, jugal, postorbital, postparietal, and
202 quadratojugal, well-mineralized Sharpey's fibers can be observed which are relatively short but
203 numerous, and sometimes packed densely in bundles. In the prefrontal, frontal, postfrontal,
204 parietal, supratemporal, squamosum, tabular and vomer, Sharpey's fibers are rare and occur

mostly in the deeper parts of the sculptural ridges (Fig. 5C). In the parasphenoid and pterygoid, Sharpey's fibers cannot be observed.

Growth marks are expressed in various ways. In the ridges of the lacrimal, frontal, jugal, postfrontal, tabular, quadratojugal and squamosum 2, they are manifested as a sequence of thin resting lines (Fig. 5D). In the postparietal, a sequence of lamellar bone layers and layers consisting of ISF are visible (Fig. 5E). In the quadratojugal, two thick annuli built up of lamellar bone alternate with two highly vascularized zones (Fig. 5F). In the postfronal, squamosum 1, supratemporal, tabular, jugal and quadratojugal, the alternations of valleys and ridges are preserved. The remains of older valleys are filled with the highly vascularized tissue which then constructed the ridges of the next generation (Fig. 5G). In the supratemporal the cementing lines indicated the remodeling process involved into the creations of sculpture is visible (Fig. 5H).

Middle region – The external cortex transits gradually into the cancellous middle region. The simple vascular canals and primary osteons, of various shapes, are mostly located next to the border between the middle and external regions. A significant part of the middle region is strongly remodeled. The few large erosion cavities (up to ~~2000 µm~~ in diameter) are present in the premaxilla, nasal, lacrimal, jugal, prefrontal, postparietal, squamosum 1, quadratojugal and all studied bones from the palatal side of the skull. The most highly remodeled middle region occurs in the vomer, where erosion cavities in some areas exceed ~~3000 µm~~ in length (Fig. 6A). In the lacrimal and prefrontal, erosion cavities reach up to the external cortex. The maxilla is dominated by numerous, but medium-sized erosion cavities. In the postfrontal, parietal and supratemporal, erosion cavities are small (less than 500 µm in diameter). In the postfrontal they appear sporadically, whereas occur numerous in parietal and supratemporal (Fig. 6B). The middle region in the tabular and squamosum 2 does not show the typical trabecular structure. The

intensive remodeling is visible; however, the tissue is relatively compact, almost without erosion cavities (Fig. 6C).

Internal cortex – The internal cortex consists of parallel-fibered to lamellar bone. The degree of vascularization varies from very low, almost avascular, in the parietal, postfrontal, supratemporal and squamosum, low in the premaxilla, prefrontal, nasal, and postparietal, moderate in the maxilla, frontal, vomer and parasphenoid, to high in the lacrimal, jugal, postorbital and quadratojugal (Fig. 6D-F). Osteocyte lacunae, showing slightly elongated shapes, are very frequent. Growth marks are visible in form of resting lines. The amount of lines varies from four in the postfrontal and parietal, three in the postparietal, supratemporal and jugal, to two in the nasale (Fig. 6D). In the parasphenoid, well developed zones and annuli can be observed (Fig. 6G). Zones are built of thick, well vascularized layers, while annuli are represented by thinner, avascular layers. The numerous Sharpey's fibers packed in bundles are visible in the tabular and vomer.

Endochondral bones

Quadrate – The partially preserved and well-vascularized cortex consists of parallel-fibered and lamellar bone (Fig. 7A, B). The simple vascular canals occur sporadically, and secondary osteons are more common (Fig. 7A, B). The Sharpey's fibers are very short and occur only in the subsurface parts of the cortex. The elongated osteocyte lacunae are present mainly within the lamellar bone, which outlines the osteons. They do not possess canaliculi. Growth marks cannot be observed.

The central region consists is of spongiosa and is characterized by large pore spaces and irregular trabeculae (Fig. 7C), which contain clumps of calcified cartilage (see also the Supplementary Material).

Exoccipital – The cortex consists of parallel-fibered bone and is relatively well-vascularized (Fig. 7D). The simple vascular are few in number (Fig. 7E, F) and located only in the outermost part of the cortex. The secondary osteons are more frequent (Fig. 7D). Well-mineralized, densely packed bundles of Sharpey's fibers are common and can be seen throughout the entire cortex (Fig. 7D, E). In the exoccipital, the Sharpey´s fibers are most abundant and pronounced among all examined bones. Rounded osteocyte lacunae are numerous. Growth marks are absent.

The central region consists of an irregular network of bony trabeculae, with large pore spaces between them (Fig. 7G). In the medial parts of the bone tissue, where trabeculae are poorly developed, accumulations of calcified cartilage are quite common (Fig. 7H).

DISCUSSION

The histological variability – Witzmann (2009) investigated fragments of dermal bones from 20 taxa and concluded that for every taxon, the bone microanatomy and histology were consistent. Intraspecific variability of the histology of dermal bones was only observed in *Mastodonsaurus giganteus* and *Plagiosternum granulosum* and only affects the degree of vascularization and remodeling of the bone (Witzmann, 2009).

Nevertheless, in the *Metoposaurus krasiejowensis* skull, the observed variability is very high and despite bones diploë structure typical for all dermal bones, can be seen in both,

microanatomical and histological levels. The bones show various thicknesses, different proportions between the layers, variations in the vascularization systems, tissue organizations, the presence and organization of Sharpey's fibers, degree of remodeling, and growth pattern (see also the Supplementary Material for the detailed description). The combination of these characters concludes that each sectioning-plane in the skull represents a unique framework. The histological properties are not related to the bone, but strictly depend on the particular sectioning-plane. The transition between the „histological types" is fluent. The jugal and postorbital, sectioned in the suture region, represent the same microanatomical and histological framework (Figs. 2 j and po, 3F; Table 1), whereas the squamosum sectioned in the frontal part of the bone (Fig. 2, sq1) and next to the otic notch (Fig. 2, sq2), showed different architecture on both microanatomical and histological levels (Figs. 3K, L). This suggests that the histological framework is not specifically bone-limited, but seems to be related to the specific area of the skull and i.e. depended on the growth of the entire skull and each bone separately, or to the local biomechanical loading on the particular part of the skull. Fortuny et al. (2012), based on the Finite Elements Analysis, showed that the hypothetical biomechanical stress along the skull is different for each skull-morphotype and depend directly on the shape of the skull and position of the orbits. If the bone framework is related to the biomechanical loading, the high variability of temnospondyls skulls results that each taxon might has a unique histological architecture of homologous bones.

Skeletochronological information – In the external cortex of the *Metoposaurus* skull, four types of growth alternation can be observed: numerous resting lines, the sequence of lamellar layers combined with the high-fibrous tissue (ISF), thick zones and annuli and the alternation of ridges and valleys (Fig. 5D-G).

In the lacrimal, frontal, jugal, postfrontal, postparietal, tabular and quadratojugal, the distinct growth marks are manifested as a sequence of numerous thin lines (Fig. 5D). Similar growth marks, present in the external and internal cortices of the dermal bone, have been observed in several temnospondyl taxa (Scheyer, 2007; Witzmann, 2009). In fast-growing amniotes, the presence of several growth lines (Line of Arrested Growth –LAG) next to the surface of bone is known as the External Fundamental System (EFS), and indicates a slowing down of growth, suggesting that the maximum size has been reached (Sander, 2000; Chinsamy-Turan, 2005; Erickson, 2005; Turvey et al., 2005; Sander et al., 2011). In *Metoposaurus* long bones, similar structures are present in the inner and outer part of the cortex, suggesting that accumulation of external resting lines does not mean the cessation of growth at all, but only the oscillation in growth rate during one season (Konietzko-Meier & Klein, 2013; Konietzko-Meier & Sander, 2013). Then, the complex with accumulation of resting lines is interpreted as the one annulus deposited during one, dry season (Konietzko-Meier & Sander, 2013; Konietzko-Meier & Klein, 2013). As in the long bones, the two highly vascularized parts of the external cortex represent the fast growing zones, and the avascular layers annuli, and the entire external cortex two growth seasons. ~~The sequences of lamellar bone and layers with accumulation of ISF visible in the postprietal (Fig. 5E) can be interpreted as three years of growth.~~ Specific growth marks also represent the alternation of valleys and ridges preserved in the postfronal, squamosum, supratemporal, trabeculare, jugal, and quadratojugal. In these bones, two generations of valleys/ridges are visible (Fig. 5G). However, for all types of growth marks, it is not known how many growth indicators have already been remodeled. In the internal cortex, two to four resting lines are visible; the only exception is the parasphenoid (Fig. 6D). The structure of the internal cortex in the parasphenoid (Fig. 6G) mostly resembles the growth sequence seen in the

318 *Metoposaurus* long bones (Konietzko-Meier & Klein, 2013; Konietzko-Meier & Sander, 2013).
319 The two thick avascular layers represent the annuli, and combined with the two high
320 vascularized zones indicate two growth seasons.

321 Due to the different number of preserved cycles in one skull the estimation of individual
322 age based on the skeletochronological information is very difficult. Without testing the whole
323 growth series, it is not possible to estimate the amount of remodeled tissue and the growth
324 pattern of each bone and thus, no direct conclusion about the individual age of sectioned skull
325 can be provided.

326 Cranial sutures were not visible on the skull surface (Gruntmejer, 2012). The
327 disappearance of all traces of sutures on the skull surface during ontogeny is a phenomena often
328 encountered in adult individuals (Moazen et al., 2008). In the completely preserved skeletons of
329 *Dutuitosaurus ouazzoui* (Dutuit, 1976), a skull of similar length (about 400 mm) as the here
330 described, corresponds with about 142 mm long femur (Dutuit, 1976: pl XXXI; personal
331 observation DKM). Steyer et al. (2004) calculated the individual age of the adult *Dutuitosaurus*
332 femur, comparable in length, for eight to nine years. For the *Metoposaurus* from Poland, large
333 femora are not known; the largest one which was studied histologically is about 90 mm long and
334 is estimated at four years of age (Konietzko-Meier & Klein, 2013). However, comparing
335 skeletochronological data of *Metoposaurus* with that of *Dutuitosaurus* revealed that the femora
336 of overlapping sizes show a similar age in both taxa, whereas the larger femora of *Dutuitosaurus*
337 are older compared to the smaller *Metoposaurus* femora (Konietzko-Meier & Klein, 2013).
338 Thus, on the basis of skeletochronology, a strong developmental plasticity can be excluded for
339 both taxa. The individual age of the Krasiejów skull, based on the comparison with
340 *Dutuitosaurus,* can be estimated at about eight to ten years. With the preservation of maximum

three growth layers in the external cortex and two in the internal one, the amount of remodeled growth marks could reach up to six to seven. This indicates a relatively fast remodeling rate of the dermal bones of the skull compared to the long bones.

Remodelling degree – Among the sections from the *Metoposaurus* skull, four main remodeling degrees could be observed in the middle region. The relatively lowest remodeled samples are from the postfrontal, parietal and supratemporal. A few large erosion cavities are present in the premaxilla, nasal, lacrimal, jugal, prefrontal, postparietal, squamosum, quadratojugal and all studied bones from the palatal side of the skull. The maxilla is dominated by numerous, but medium sized erosion cavities. In the middle region of the tabular and squamosum 2, the bone deposition exceeds the bone resorption and it does not represent the typical spongious structure.

The increase in remodeling degree is known as a one of the developmental characters. Witzmann (2009) published the detailed histology of dermal bones from a young adult and adult *Mastodonsaurus,* and observed an increase in remodeling (expressed as an increase of the erosion cavities sizes) in the older specimen. In the *Metoposaurus* skull, different histological stages can be observed among different bones in the skull. The low (postfrontal, parietal and supratemporal) and highly (premaxilla, nasal, lacrimal, jugal, prefrontal, postparietal, squamosum, quadratojugal) remodeled bones seem to represent two stages of the same process, resulting in the increase in porosity of the middle region. This may indicate the sequence of the skull ossification during ontogeny, with the latest ossification of bones occurring on the central part of the skull roof. However, less remodeled samples originate from the groves-ridges regions, whereas the other sections come from the reticulate areas. This ~~confirms~~ the hypothesis presented first by Bystrow (1935) that the polygonal reticulate structures are the center of

ossification and ridges-grooves areas show the direction and extent of growth from theses ossification centers. In this case, different remodeling degrees, which resemble the ontogenetic change, is the result of longitudinal growth of the bone.

Dynamic of the sculpture pattern – Although dermal sculpture was early recognized as a characteristic for basal tetrapods (e.g. von Meyer, 1858; Fraas, 1889; Fritsch, 1889; Zittel, 1911), the morphogenesis of the sculptures is still questionable (summarized by Witzmann et al., 2010, de Buffrénil et al., 2016). Among extant tetrapods, growth of dermal bony tubercles and ridges has been studied in osteoderms of squamates and in dermal skull bones and osteoderms of crocodiles. In squamates, the presence of pits and ridges on the external surface of osteoderms follows from both local resorption and growth of bone (Zylberberg and Castanet, 1985; Levrat-Calviac & Zylberberg, 1986), whereas in crocodile dermal bones, de Buffrénil (1982) stated that sculpture is mainly the result of local resorption. In contrast, Vickaryous and Hall (2008) found no evidence for morphogenesis of bone sculpture by resorption in *Alligator mississippiensis* and presumed that sculptural ridges develop by preferential bone growth. Concerning basal tetrapods, Bystrow (1935, 1947) showed that the development of bone sculpture in the temnospondyls *Benthosuchus*, *Platyoposaurus* and *Dvinosaurus* took place solely by growth of the bony ridges and tubercles, and resorptive processes were not involved. The thin sections of the dermal bones of skull and pectoral girdle in the basal tetrapods investigated by Witzmann (2009), corroborate Bystrow's findings and show that the dermal sculpture did not develop by local resorption of the bone surface, comparable to the pattern in basal tetrapod osteoderms (Witzmann & Soler-Gijón 2008). According to the last study (de Buffrénil et al., 2016) the involvement of several complex remodeling processes, with the local succession of resorption and reconstruction cycles, is frequent and occurs in all major gnathostome clades. All temnospondyl sections share an

387 important common feature: the lack of superficial remodeling (resorption and reconstruction
388 cycles). The supratemporal of *Metoposaurus* however show the clearly remodeling process
389 involved into the sculpture creation (Fig. 5H). Because of it is the only one sample it is difficult
390 to generalize the observation, but it proofs that the osteogenic mechanisms involved in the
391 creation and growth are still not clear.
392 The latest study of de Buffrénil et al. (2016) confirmed, however, that the distinct dynamic
393 processes are involved in the creation and growth of pits and ridges. Authors (de Buffrénil et al.,
394 2016) observed six main patterns of modification of ornamentation image during growth. The
395 simplest one is repetition of the width or position of pits and ridges from one growth stage to the
396 following one. The ridges can drift diverge symmetrically in two opposite directions or the
397 ridges around a given pit may migrate in the same direction. Also the change of size of the ridges
398 is possible providing to the gradual narrowing of pit diameter (convergent ridge drift) or opposite
399 process may occur when the reduction of ridge width is observed. In most drastic case the pits
400 can be entirely filled, and disappear to be replaced in situ by ridges.
401 The sections from the *Metoposaurus* skull show that the new bone deposition mostly
402 repeats the pattern of sculptures present in the younger stages (Fig. 5D-F); but an ridges drift and
403 valley/ridges alternation my also occur (Fig. 5G). In the last case in such places, where valleys
404 occurred, ridges are being deposited during the next bone generation stage. However, the
405 distance between newly created tops of the ridges is not distinctively different than of the
406 previous generation.
407 It indicates that the metric pattern of the sculpture is relatively stable, but the position of
408 the ridges and grooves is dynamic during growth as a specific adaptation to different
409 biomechanical loading on the new, larger bone.

Sharpey's fibers – The well-mineralized Sharpey's fibers are present in the cortex of all bones of the *Metoposaurus krasiejowensis* skull. In dermal bones, they are most likely the remains of soft tissue and small muscle attachments (Francillion-Vieillot et al., 1990). In the occipital condyles, Sharpey's fibers are densely packed in bundles and they are much thicker and longer (Fig. 7D) than in the other bones. The Sharpey's fibers occur here in similar amounts like in vertebrae (Konietzko-Meier et al., 2013). Large concentrations of Sharpey's fibers indicate that the exoccipital creates an attachment point for well developed, strong muscles and ligaments which connects the skull to the vertebral column.

Quadrate bone and exoccipital – These bones clearly differ from all other bones of the skull. Their internal structure is very similar to vertebral intercentra. In the case of *Metoposaurus krasiejowensis*, the histology and ossification process of the vertebrae have been detailed described (Konietzko-Meier et al., 2013). The quadrate and exoccipital consists of a trabecular middle region, surrounded by a thin layer of well-vascularized cortex. The presence of cartilage (Fig. 7H) indicates that ossification follows a pattern known for vertebrae with relatively slow ossification of the trabecular part and late development of the periosteal cortex (Konietzko-Meier et al., 2013).

ACKNOWLEDGEMENST

The authors acknowledge Olaf Dülfer (University of Bonn, Steinman Institute) for preparing some of the thin-sections. We are grateful to Kayleigh Wiersma (University of Bonn, Steinmann

Institute) for improving the English. Aurore Canoville and Martin Sander are acknowledged for fruitful discussion. We thank both reviewers (…..) and editors for all comments.

Author Contributions

Conceived and designed the experiments: KG DKM AB. Analyzed the data: DKM KG AB. Contributed reagents/materials/analysis tools: DKM KG AB. Wrote the paper: DKM KG AB.

REFERENCES

1. Bodzioch A, Kowal-Linka M. 2012. Unraveling the origin of the Late Triassic multitaxic bone accumulation at Krasiejow (S Poland) by diagenetic analysis. *Palaeogeography, Palaeoclimatology, Palaeoecology* 346/347:25-36.
2. Brusatte SL, Nesbitt SJ, Irmis RB, Butler RJ, Benton MJ, Norell MA. 2010. The origin and early radiation of dinosaurs. *Earth-Science Reviews* 101:68-100.
3. Brusatte SL, Butler MJ, Mateus O, Steyer JS. 2015. A new species of *Metoposaurus* from the Late Triassic of Portugal and comments on the systematics and biogeography of Metoposaurid Temnospondyls. *Journal of Vertebrate Paleontology*, 35(3): e912988, DOI: 10.1080/02724634.2014.912988.
4. Buffrénil de V. 1982. Morphogenesis of bone ornamentation in extant and extinct crocodilians. *Zoomorphology* 99(2):155-166.

5. Buffrénil de V, Clarac F, Canoville A, Laurin M. 2016. Comparative data on the differentiation and growth of bone ornamentation in Gnathostomes (Chordata: Vertebrata). *Journal of Morphology* (in press.).
6. Bystrow AP, 1935. Morphologische Untersuchungen der deckknochen Schädels der Stegocephalen. *Acta Zoologica* 16:65-141.
7. Bystrow AP. 1947. Hydrophilous and zenophilous labyrinthodonts. *Acta Zoologica* 28:137-164.
8. Castanet J, Francillon-Vieillot H, de Ricqlès A. 2003. The skeletal histology of the Amphibia. In H. Heatwole and M. Davies (eds.), Amphibian Biology, Volume 5, Osteology. Surrey Beatty and Sons, Chipping Norton, New South Wales, Australia, 1598-1683.
9. Chinsamy-Turan A. 2005. The Microstructure of Dinosaur Bone: Deciphering Biology with Fine-scale Techniques. Johns Hopkins University Press, Baltimore. 1-195.
10. Coldiron RW. 1974. Possible functions of ornament in labyrinthodont amphibians. *Occasional Papers of the Museum of Natural History of the University of Kansas*, Lawrence, 33:1-19.
11. Dutuit JM. 1976. Introduction à l'etude paleontologique du Trias continental marocain. Description des premiers Stegocephales recueillis dans le couloir d'Argana (Atlas occidental). *Memoires du Museum National d'Histoire Naturelle Paris Ser. C* 36:1-253.
12. Dzik J, Sulej T, Kaim A, Niedźwiedzki R. 2000. Późnotriasowe cmentarzysko kręgowców lądowych w Krasiejowie na Śląsku Opolskim. *Przegląd Geologiczny* 48:226-35.

13. Dzik J. 2001. A new *Paleorhinus* fauna in the early Late Triassic of Poland. *Journal of Vertebrate Paleontology* 21:625-627.

14. Dzik J. 2003. A beaked herbivorous archosaur with dinosaur affinities from the early Late Triassic of Poland. *Journal of Vertebrate Paleontology* 23:556-574.

15. Dzik J, Sulej T. 2007. A review of the early Late Triassic Krasiejów biota from Silesia, Poland. *Palaeontologia Polonica* 64:3-27.

16. Dzik J. 2008. Gill structure and relationships of the Triassic cycloid crustaceans. *Journal of Morphology* 269:1501-1519.

17. Enlow DH, Brown SO. 1956. A comparative histological study of fossil and recent bone tissues. *I. Texas Journal of Science* 8:405-43.

18. Erickson GM. 2005. Assessing dinosaur growth patterns: a microscopic revolution. *Trends in Ecology and Evolution* 20(12):677-84.

19. Fortuny J, Marcé-Nogué J, de Esteban-Trivigno S, Gil L, Galobart Á. 2011. Temnospondyli bite club: ecomorphological patterns of the most diverse group of early tetrapods. *Journal of Evolutionary Biology* 24:2040-2054.

20. Fortuny J, Marce´-Nogue´ J, Gil L, Galobart A`. 2012. Skull mechanics and the evolutionary patterns of the otic notch closure in Capitosaurs (Amphibia: Temnospondyli). *The Anatomical Record* 295:1134-1146.

21. Fraas E. 1889. Die Labyrinthodonten der Schwäbischen Trias. *Palaeontographica* 36:1-158.

22. Francillon-Vieillot H, de Buffrénil V, Castanet J, Géraudie J, Meunier F-J, Sire J-Y, Zylberberg L, de Ricqlès A. 1990. Microstructure and mineralization of vertebrate

497 skeletal tissues. In: Carter JG [ed.]: Skeletal Biomineralization: Patterns, Processes and
498 Evolutionary Trends, Vol. I. Van Nostrand Reinhold, New York. 471-530.
499 23. Fritsch A. 1889. Fauna der Gaskohle und der Kalksteine der Permformation Böhmens,
500 Vol. 2. Prag: Selbstverlag. 1-132.
501 24. Gądek K. 2012. Palaeohistology of ribs and clavicle of *Metoposaurus diagnosticus* from
502 Krasiejów (Upper Silesia, Poland). *Opole Scientific Society Nature Journal* 45:39-42.
503 25. Gross W. 1934. Die Typen des mikroskopischen Knochenbaues bei fossilen
504 Stegocephalen und Reptilien. *Zeitschrift für Anatomie und Entwicklungsgeschichte*
505 203:731-64.
506 26. Gruntmejer K. 2012. Morphology and function of cranial sutures of the Triassic
507 amphibian *Metoposaurus diagnosticus* (Temnospondyli) from southwest Poland. In: Jagt-
508 Yazykova E, Jagt J, Bodzioch A, & Konietzko-Meier D. [eds] Krasiejów –
509 palaeontological inspirations. *ZPW Plik*, Bytom. 34-54.
510 27. Gruszka B, Zieliński T. 2008. Evidence for a very low-energy fluvial system: a case
511 study from the dinosaur-bearing Upper Triassic rocks of Southern Poland. *Geological*
512 *Quarterly* 52:239-252.
513 28. Konietzko-Meier D, Sander PM. 2013 Longe bone histology of Metoposaurus
514 diagnosticus (Temnospondyli) from the Late Triassic of Krasiejów (Poland) and its
515 paleobiological implications. *Journal of Vertebrate Paleontology* 35(5):1-16.
516 29. Konietzko-Meier D, Klein N. 2013. Unique growth pattern of *Metoposaurus diagnosticus*
517 *krasiejowensis* (Amphibia, Temnospondyli) from the Upper Triassic of Krasiejów,
518 Poland. *Palaeogeography Palaeoclimatology Palaeoecology* 370:145-157.

519 30. Konietzko-Meier D, Bodzioch A, Sander PM, 2013. Histological characteristics of the
520 vertebral intercentra of *Metoposaurus diagnosticus* (Temnospondyli) from the Upper
521 Triassic of Krasiejów (Upper Silesia, Poland). *Earth and Environmental Science*
522 *Transactions of the Royal Society of Edinburgh* 103:1-14.
523 31. Konietzko-Meier D, Danto M, Gądek K, 2014. The microstructural variability of the
524 intercentra among temnospondyl amphibians. *Biological Journal of the Linnean Society*
525 112:747-764.
526 32. Levrat-Calviac V, Zylberberg L. 1986. The structure of the osteoderms in the gekko:
527 *Tarentola mauritanica*. *American Journal of Anatomy* 176:437-446.
528 33. Lucas SG. 2015. Age and correlation of Late Triassic tetrapods from southern Poland.
529 *Annales Societatis Geologorum Poloniae* 85(4):627-635.
530 34. Lucas SG, Spielmann JA, Hunt AP. 2007. Bio-chronological significance of Late Triassic
531 tetrapods from Krasiejów, Poland. *New Mexico Museum of Natural History and Science*
532 *Bulletin* 41:248-258.
533 35. Meyer E. 1842. Labyrinthodonten—Genera. Neues Jahrbuch für Mineralogie,
534 *Geographie, Geologie, Palaeontologie* 1842:301-304.
535 36. Meyer H von. 1858. Reptilien aus der Steinkohlenformation in Deutschland.
536 *Palaeontographica* 6:59-219.
537 37. Moazen M, Curtis N, Evans SE, O'Higgins P, Fagan M.J. 2008. Rigid-body analysis of a
538 lizard skull: Modelling the skull of *Uromastyx hardwickii*. *Journal Biomechanics*
539 41:1274-1280.

38. Mukherjee D, Ray S, Sengupta DP. 2010. Preliminary observations of the bone microstructure, growth patterns, and life habits of some Triassic Temnospondyls from India. *Journal of Vertebrate Paleontology* 30(1):78-93.

39. Olempska E. 2004. Late Triassic spinicaudatan crustaceans from southwestern Poland. *Acta Palaeontologica Polonica* 49(3):429-442.

40. Olempska E. 2011. Fresh-water ostracods from the Late Triassic of Poland. *Joannea Geologie und Paläontologie* 11:154-155.

41. Lamm ET. 2014. Preparation and sectioning of specimens. In: Padian K, Lamm ET, (eds.), Bone histology of fossil tetrapods, advancing methods, analysis, and interpretation. University of California Press. Barkley, Los Angeles, London. 35-54.

42. Racki G, Szulc J. 2014. Formacja grabowska – podstawowa jednostka litostratygraficzna kajpru Górnego Śląska. *Przegląd Geologiczny* 63(2):103-113.

43. Ricqlès A. de 1981. Recherches paléohistologiques sur les os longs des tétrapodes. VI.- Stégocéphales. *Annales de Paléontologie* 67:141-160.

44. Rienhart LF, Lucas SG, 2013. The functional morphology of dermal bone ornamentation in temnospondyl amphibian. In: Tanner LH, Spielmann JA & Lucas SG [eds] The Triassic System. New Mexico Museum of Natural History and Science, Bulletin 61. 524-532.

45. Sanchez S, Germain D, de Ricqlès, Abourachid A, Goussard F, Tafforeau P, 2010. Limb-bone histology of temnospondyls: implications for understanding the diversification of palaeoecologies and patterns of locomotion of Permo-Triassic tetrapods. *Journal of Evolutionary Biology* 1-15.

562 46. Sander PM. 2000. Long bone histology of the Tendaguru sauropods: implications for
563 growth and biology. *Paleobiology* 26:466-488.
564 47. Sander PM, Klein N, Stein K, Wings O. 2011. Sauropod bone histology and its
565 implications for sauropod biology. In Klein N, K. Remes K, Gee C T & Sander PM [eds]
566 Biology of the Sauropod Dinosaurs: Understanding the Life of Giants. Life of the Past
567 (series ed. J. Farlow). Indiana University Press, Bloomington. 276-302
568 48. Scheyer TM. 2007: Skeletal histology of the dermal armor of Placodontia: the occurrence
569 of 'postcranial fibro-cartilaginous bone' and its developmental implications. *Journal of*
570 *Anatomy* 211:737-753.
571 49. Schoch RR. 1999. Comparative osteology of *Mastodonsaurus giganteus* (Jaeger, 1828)
572 from the Middle Triassic (Lettenkeuper: Longobardian) of Germany (Baden-
573 Württemberg, Bayern, Thüringen). *Stuttgarter Beiträge zur Naturkunde Serie B*
574 *(Geologie und Paläontologie)* 278:1-170.
575 50. Schoch RR, Milner AR. 2000. Stereospondyli. *Handbuch der Palaeoherpetologie* 3B.
576 Munich: Verlag Dr. Friedrich Pfeil 1-230.
577 51. Skawina A, Dzik J. 2011. Umbonal musculature and relationships of the Late Triassic
578 filibranch unionoid bivalves. *Zoological Journal of the Linnean Society* 163:863-883.
579 52. Skawina A. 2013. Population dynamics and taphonomy of the Late Triassic (Carnian)
580 freshwater bivalves from Krasiejów (Poland). *Palaeogeography, Palaeoclimatology,*
581 *Palaeoecology* 379:68-80.
582 53. Skrzycki P. 2015. New species of lungfish (Sarcopterygii, Dipnoi) from the Late Triassic
583 Krasiejów site in Poland, with remarks on the ontogeny of Triassic dipnoan tooth plates.
584 *Journal of Vertebrate Paleontology* 35(5):e964357.

54. Steyer JS, Laurin M, Castanet J, de ~~Ricqle`s~~ A. 2004. First histological and skeletochronological data on temnospondyl growth: palaeoecological and palaeoclimatological implications. *Palaeogeography, Palaeoclimatology, Palaeoecology* 206:193-201.

55. Sulej T, 2002. Species discrimination of the Late Triassic temnospondyl amphibian Metoposaurus diagnosticus. *Acta Paleontologia Polonica* 47(3):535-546.

56. Sulej T. 2005. A new rauisuchian reptile (Diapsida: Archosauria) from the Late Triassic of Poland. *Journal of Vertebrate Paleontology* 25(1):78-86.

57. Sulej T, Majer D. 2005. The temnospondyl amphibian *Cyclotosaurus* from the Upper Triassic of Poland. *Palaeontology* 48:157-170.

58. Sulej T. 2007: Osteology, variability, and evolution of *Metoposaurus*, a temnospondyl from the Late Triassic of Poland. *Paleontologia Polonica* 64:29-139.

59. Sulej T. 2010. The skull of an early Late Triassic aetosaur and the evolution of the stagonolepidid archosaurian reptiles. *Zoological Journal of the Linnean Society* 158:860-881.

60. Szulc J, Racki G, Jewuła K. 2015a. Key aspects of the stratigraphy of the Upper Silesian middle Keuper, southern Poland. *Annales Societatis Geologorum Poloniae* 85(4):557-586.

61. Szulc J, Racki G, Jewuła K, Środoń J. 2015b. How many Upper Triassic bone–bearing levels are there in Upper Silesia (southern Poland)? A critical overview of stratigraphy and facies. *Annales Societatis Geologorum Poloniae* 85(4):587-626.

62. Turvey SP, Green OR, Holdaway RN. 2005. Cortical growth marks reveal extended juvenile development in New Zealand moa. *Nature* 435:940-943.

608 63. Vickaryous MK, Hall BK. 2008. Development of the dermal skeleton in *Alligator*
609 *mississippiensis* (Archosauria, Crocodylia) with comments on the homology of
610 osteoderms. *Journal of Morphology* 269:398-422.
611 64. Witzmann F, Soler-Gijón R. 2008. The bone histology of osteoderms in temnospondyl
612 amphibians and in the chroniosuchian *Bystrowiella*. *Acta Zoologica* (Stockholm) 91: 96-
613 114. DOI 10.1463–6395.1111/j2008.00385.x
614 65. Witzmann F. 2009. Comparative histology of sculptured dermal bones in basal tetrapods,
615 and the implications for the soft tissue dermis. *Palaeodiversity* 2:233-270.
616 66. Witzmann F, Scholz H, Müller J, Kardjilov N. 2010. Sculpture and vascularization of
617 dermal bones, and the implications for the physiology of basal tetrapods. *Zoological*
618 *Journal of the Linnean Society* 160:302-340.
619 67. Zittel KA. 1911. Grundzüge der Paläontologie (Paläozoologie). II. Abteilung. Vertebrata.
620 Verlag von R. Oldenbourg, München and Berlin. 1-589.
621 68. Zylberberg L, Castanet J. 1985. New data on the structure and the growth of the
622 osteoderms in the reptile *Anguis fragilis* L. (Anguidae, Squamata). *Journal of*
623 *Morphology* 186:327-342.
624
625
626
627
628
629
630

631

632

633 **Fig. 1.** The skull of *Metoposaurus krasiejowensis* (UOPB 01029) from Late Triassic of Poland.
634 **(A)** Dorsal view of skull; **(B)** Ventral view of the skull. Scale bar equals 10 cm.

635

636 **Fig. 2.** The sectioning planes of the *Metoposaurus krasiejowensis* skull (UOPB 01029) from
637 Late Triassic of Poland. **(A)** The skull roof; **(B)** The palatal side of the skull. The sectioning
638 planes are marked by red lines. Dark grey color indicates preserved parts of the skull; the
639 destroyed or sediment-covered regions are indicated by the light grey color. Scale bar equals 10
640 cm. Abbreviations: pm = premaxilla, m = maxilla, n = nasal, l = lacrimal, prf = prefrontal, j =
641 jugal, po = postorbital, pf = postfrontal, f = frontal, p = parietal, st = supratemporal, sq1 =
642 squamosum 1, sq2 = squamosum 2, pp = postparietal, t = tabular, qj = quadratojugal, v = vomer,
643 ps = parasphenoid, pt = pterygoid, q = quadrate bone, ex = exoccipital.

644

645 **Fig. 3.** General microanatomy of the skull bones of *Metoposaurus krasiejowensis* (UOPB 01029)
646 from Late Triassic of Poland. **(A)** premaxilla; **(B)** maxilla; **(C)** nasal; **(D)** lacrimal; **(E)**
647 prefrontal; **(F)** jugal/ postorbital; **(G)** postfrontal; **(H)** frontal; **(I)** parietal; **(J)** supratemporal; **(K)**
648 squamosum 1; **(L)** squamosum 2; **(M)** postparietal; **(N)** tabular; **(O)** quadratojugal; **(P)**
649 parasphenoid; **(Q)** vomer; **(R)** pterygoid; **(S)** quadrate bone; **(T)** exoccipital. Scale bar equals 10
650 mm. Abbreviations: ap = alary process, ds = dental shelf, vp = vomeral process.

651

652 **Fig. 4.** Detailed microanatomy of the skull bones of *Metoposaurus krasiejowensis* (UOPB
653 01029) from Late Triassic of Poland, based on the frontal. **(A)** A valley and two ridges; **(B)**

654 Enlargement of (A); the external and internal cortex, and trabecular middle region with
655 numerous and large erosion cavities are visible; image in cross-polarized light; **(C)** The same as
656 (B), but in plane-polarized light. Dashed lines mark the approximately border between the
657 external cortex/middle region/internal cortex. Scale bars equal 10 mm for (A), and 500 µm for
658 (B-C). Abbreviations: g = groove, v = valley, EC = external cortex, MR = middle region, IC =
659 internal cortex, ER = erosion cavities, LB = lamellar bone, PFB = parallel-fibred bone.
660

661 **Fig. 5.** Histology of the external cortex of the skull bones of *Metoposaurus krasiejowensis*
662 (UOPB 01029) from Late Triassic of Poland. **(A)** Fragment of external cortex of the frontal,
663 image in plane-polarized light; **(B)** Same as (A), but in cross-polarized light; **(C)** External cortex
664 of the tabular with distinct Sharpey's fibers in the area of the sculptural ridges, image in cross-
665 polarized light; **(D)** The resting lines (black arrows) in the cortex of squamosum2, image in
666 plane-polarized light; **(E)** The resting lines expressed as an alternation of lamellar layers and
667 layers with distinct Interwoven Structural Fibers (ISF) in the external cortex of the postparietal,
668 image in cross-polarized light; **(F)** Zones and annuli present in the external cortex of the
669 quadratojugal, image in cross-polarized light; **(G)** Alternation of valleys and ridges in the
670 postfrontal, image in cross-polarized light; note that remains of lamellar bone in the deep part of
671 cortex are present, representing the bottom of a valley from an older generation. **(H)** The
672 cementing lines (black arrows) visible in the superficial part of the external cortex of the
673 supratemporal. Dashed lines mark the approximate border between the external cortex/middle
674 region/internal cortex. Scale bars equal for (A-E) and (H) 100 µm and for (F)-(G) 500 µm.
675 Abbreviations: OL = osteocyte lacunae, FLB = fibro-lamellar bone, PO = primary osteons, SF =

Sharpey's fibers, ~~LB = lamellar bone,~~ ISF = Interwoven Structural Fibers, A = annulus, Z = zone, r = ridge, v = valley.

Fig. 6. The details of the histology of the middle region and internal cortex of the skull (UOPB 01029) bones of *Metoposaurus krasiejowensis* from Late Triassic of Poland. **(A)** Large erosion cavities present in the middle region of the vomer; image in plane-polarized light; **(B)** Poorly remodeled, well vascularized middle region of the parietal; image in plane-polarized light; **(C)** Poorly vascularized fragment of the middle region of the squamosum2; image in plane-polarized light; **(D)** Avascular internal cortex with resting lines (black arrows) visible in the parietal; image in plane-polarized light; **(E)** Moderately vascularized internal cortex of the premaxilla; image in plane-polarized light; **(F)** Highly vascularized internal cortex of the jugal; image in plane-polarized light; **(G)** Alternation of thick annuli and zones visible in the internal cortex of the parasphenoid; image in cross-polarized light. Dashed lines mark the approximately border between the external cortex/middle region/internal cortex. Scale bars equal 100 μm for (D) and (G) and 500 μm for other photographs. Abbreviations: IC = internal cortex, MR = middle region, EC = external cortex, VC = vascular canals, A = annulus, Z = zone.

Fig. 7. Histological details of the quadratum (A-C) and exooccipitale (D-H) of *Metoposaurus krasiejowensis* skull (UOPB 01029) from Late Triassic of Poland. **(A)** Fragment of cortex of the quadratum; image in plane-polarized light; **(B)** The same as (A), but in cross-polarized light; **(C)** Trabecular bone of the quadrate bone; image in plane-polarized; **(D)** Fragment of cortex of the exooccipitale with distinct Sharpey's fibers; image in cross-polarized light; **(E)** Close-up of (D), note that the Sharpey's fibers are also visible in plane-polarized light; **(F)** The same as (E) but in

699 cross-polarized light; **(G)** Trabeculae visible in the central part of the exooccipitale, image in
700 plane-polarized light; **(H)** Remains of calcified cartilage preserved in the trabeculae part of
701 exoccipital, image in cross-polarized light. Scale bars equal 500 μm for (C), (D) and (G), and
702 100 μm for other photographs. Abbreviations: C = cortex, TR= trabecular region, OL = osteocyte
703 lacunae, PO = primary osteons, PFL = parallel-fibred bone, VC = vascular canals, ER = erosion
704 cavities, SO = secondary osteons, SF = Sharpey's fibers, CC = calcified cartilage.
705

Table 1(on next page)

Microanatomy of the sampled bones of Metoposaurus krasiejowensis[i] skull (UOPB 01029).

1 Microanatomy of the sampled bones of *Metoposaurus krasiejowensis* skull (UOPB 01029).

bone	ornamentation	min-max thickness (µm)	average thickness (µm)[1]	E:M:I[2]	thickness of the external cortex (µm)
premaxilla (pm)	not preserved	3000 - 5000	4081.2	1:5.4:0.6	583.0
maxilla (m)	not preserved	4000-12000	10720.0	1:11.8:0.6	800.0
nasal (n)	relatively high ridges (about 1000 µm)	1000-8000	1404.0	1:3.6:0.6	270.0
lacrimal (l)	medium high (500 µm), steep ridges and wide grooves	2250-8000	2790.0	1:7.5:0.8	300.0
prefrontal (prf)	medium high (500 µm) and steep ridges	4000-6000	5022.0	1:3.7:0.7	930.0
jugal (j)	high ridges (about 1000 µm) and wide grooves	4000-6500	5900	1:4.2:0.7	1000.0
postorbital (po)	high ridges (about 1000 µm) and wide grooves	4000-6500	5900	1:4.2:0.7	1000.0
postfrontal (pf)	low ridges (about 300 µm) and shallow grooves	3000-5000	3212.0	1:5.7:0.6	440.0
frontal (f)	high ridges (about 1000 µm) and wide grooves	4000-5000	4686.0	1:5.5:0.6	660.0
parietal (p)	high ridges (about 1000 µm) and narrow pits	1000-4000	1960.0	1:3.5:0.4	400.0
supratemporal (st)	high ridges (about 1500 µm) and wide grooves	3000-5000	5130.0	1:4.4:0.3	900.0
squamosum 1 (sq1)	very high ridges (up to 2000 µm) and wide grooves	3000-7000	4700.0	1:2.2:0.2	1100.0
squamosum 2 (sq2)	high ridges (about 1000 µm) and wide grooves	1200-3900	3050.0	1:0.3:0.5	1750.0
postparietal (pp)	steep, high ridges (about 1500 µm) and polygonal pits	7500-10500	6020.0	1:3.1:0.2	1400.0
tabular (t)	high ridges (about	10000-	9760.0	1:6.5:0.8	1000.0

	1000 μm) and wide pits	12000			
quadratojugal (qj)	high ridges (about 1000 μm) and wide grooves	5000-7000	5100.0	1:2.9:0.6	900.0
vomer (v)	no clear sculpture	3000-6000	3379.0	1:2.8:0.7	650.0
parasphenoid (ps)	no clear sculpture	2000-5000	3750.0	1:5:1.5	900.0
pterygoid (pt)	no clear sculpture	5500-8000	5750.0	1:5.4:1	550.0
quadrate bone (q)*	-	diameter 20 mm			
exoccipital (ex)*	-	diameter 20 mm			

[1]The average thickness of entire bone was estimated in thin sections, expressed as an arithmetical average from three measurements of the thickness of a bone taken on the bottom of valleys and the top of ridges;[2] For the estimation of ratio between external cortex (E), medial region (M) and internal cortex (I): E:M:I, the thickness of external cortex was taken as one and then proportionally the value for medial region and internal cortex were calculated;

*Non-dermal bone

Figure 1(on next page)

The skull of Metoposaurus krasiejowensis [i](UOPB 01029) from Late Triassic of Poland.

(A) **Dorsal view of skull; (B)** Ventral view of the skull. Scale bar equals 10 cm.

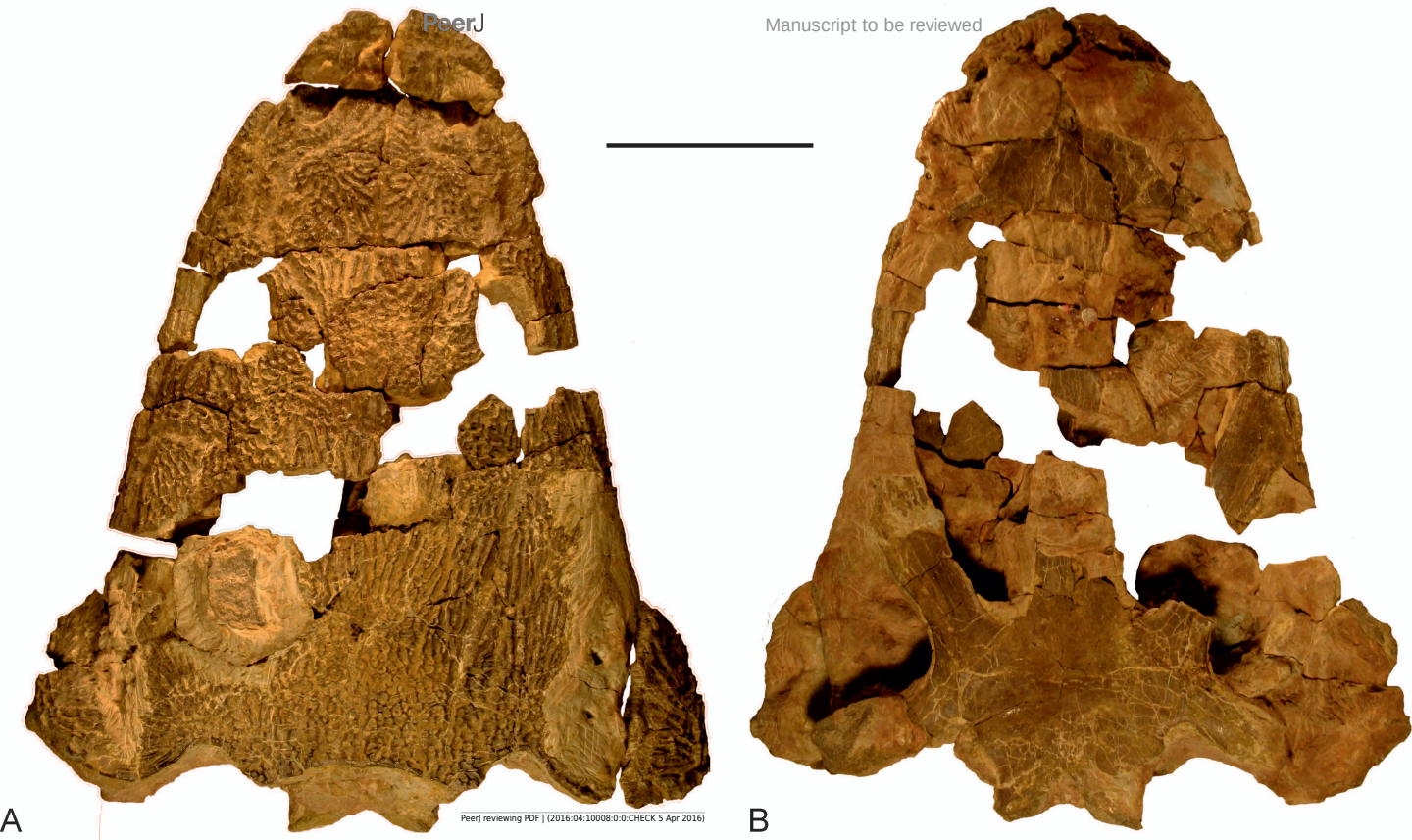

A

B

Figure 2(on next page)

The sectioning planes of the Metoposaurus krasiejowensis[i] skull (UOPB 01029) from Late Triassic of Poland.

(A) **The skull roof; (B)** The palatal side of the skull. [b]The sectioning planes are marked by red lines. Dark grey color indicates preserved parts of the skull; the destroyed or sediment-covered regions are indicated by the light grey color. Scale bar equals 10 cm. Abbreviations: pm = premaxilla, m = maxilla, n = nasal, l = lacrimal, prf = prefrontal, j = jugal, po = postorbital, pf = postfrontal, f = frontal, p = parietal, st = supratemporal, sq1 = squamosum 1, sq2 = squamosum 2, pp = postparietal, t = tabular, qj = quadratojugal, v = vomer, ps = parasphenoid, pt = pterygoid, q = quadrate bone, ex = exoccipital.

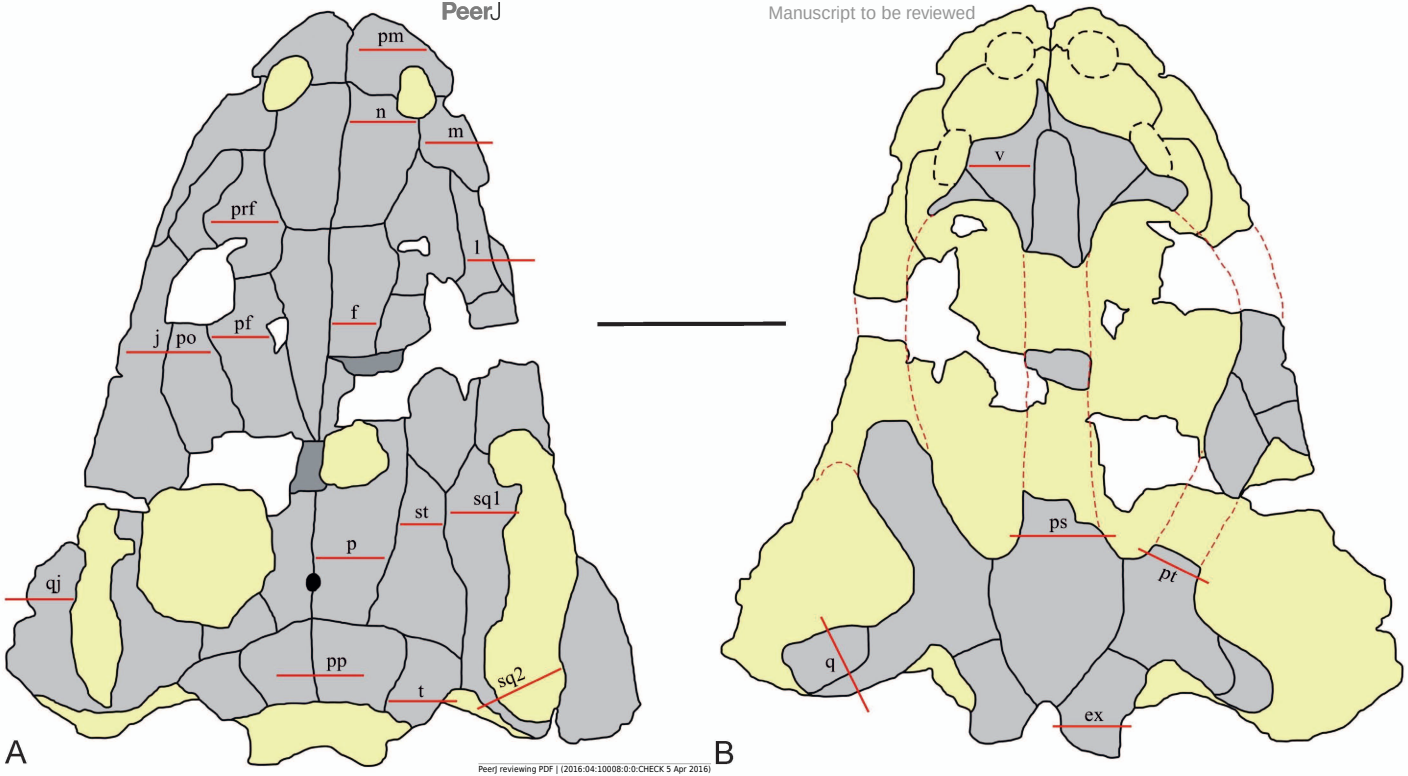
pm
n
m
prf
l
f
j
po
pf
st
sq1
p
qj
pp
t
sq2
A
v
ps
pt
q
ex
B

Figure 3(on next page)

General microanatomy of the skull bones of Metoposaurus krasiejowensis[i] (UOPB 01029) from Late Triassic of Poland.

(A) **premaxilla; (B)** maxilla; (C) **nasal; (D)** lacrimal; (E) **prefrontal; (F)** jugal/ postorbital; (G) **postfrontal; (H)** frontal; (I) **parietal; (J)** supratemporal; (K) **squamosum 1; (L)** squamosum 2; (M) **postparietal; (N)** tabular; (O) **quadratojugal; (P)** parasphenoid; (Q) **vomer; (R)** pterygoid; (S) **quadrate bone; (T)** exoccipital. Scale bar equals 10 mm. Abbreviations: ap = alary process, ds = dental shelf, vp = vomeral process.

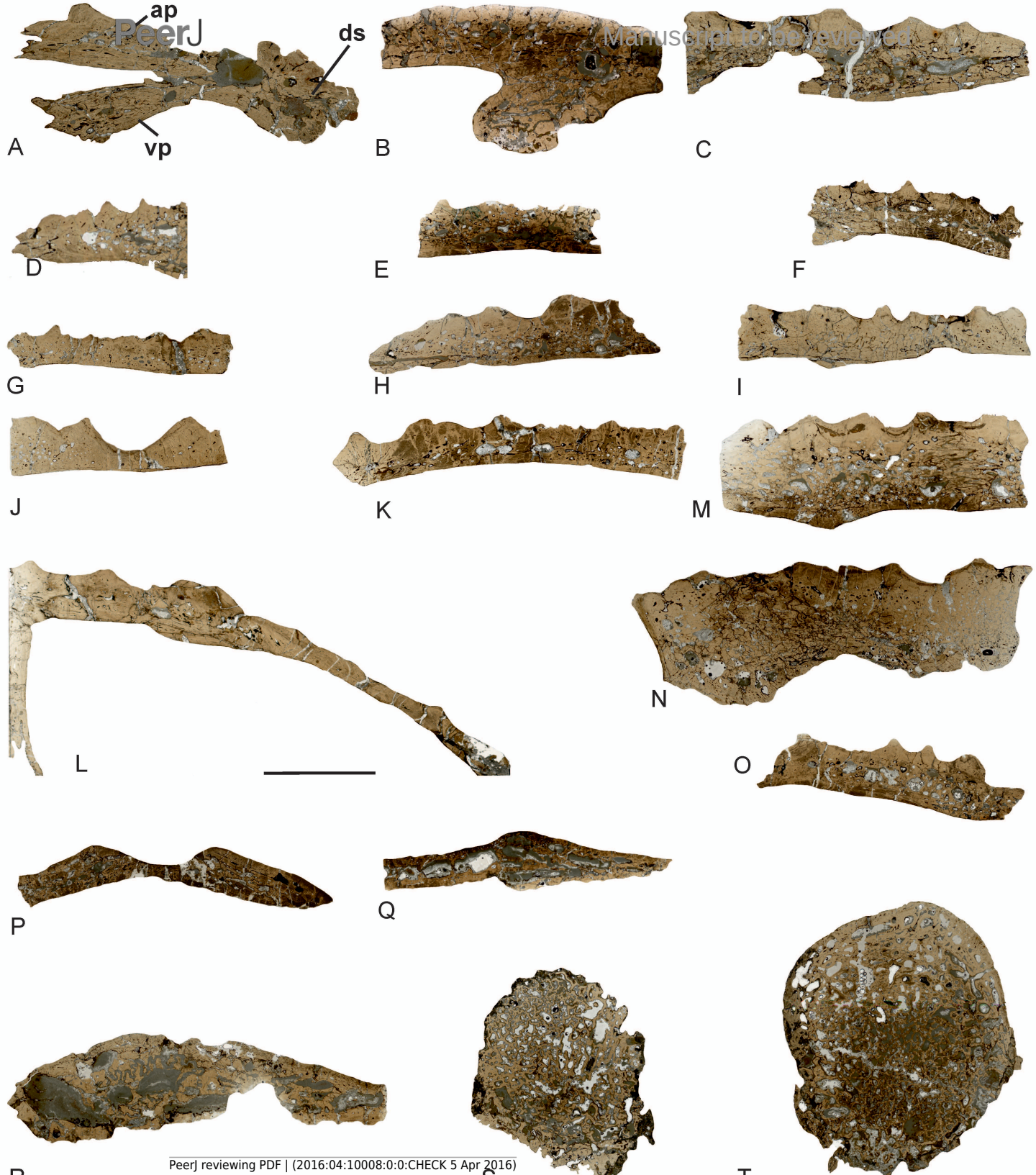

Figure 4(on next page)

Detailed microanatomy of the skull bones of Metoposaurus krasiejowensis ([i]UOPB 01029) from Late Triassic of Poland, based on the frontal.

(A) **A valley and two ridges; (B)** Enlargement of (A); the external and internal cortex, and trabecular middle region with numerous and large erosion cavities are visible; image in cross-polarized light; (C)[b] The same as (B), but in plane-polarized light. Dashed lines mark the approximately border between the external cortex/middle region/internal cortex. Scale bars equal 10 mm for (A), and 500 µm for (B-C). Abbreviations: g = groove, v = valley, EC = external cortex, MR = middle region, IC = internal cortex, ER = erosion cavities, LB = lamellar bone, PFB = parallel-fibred bone.

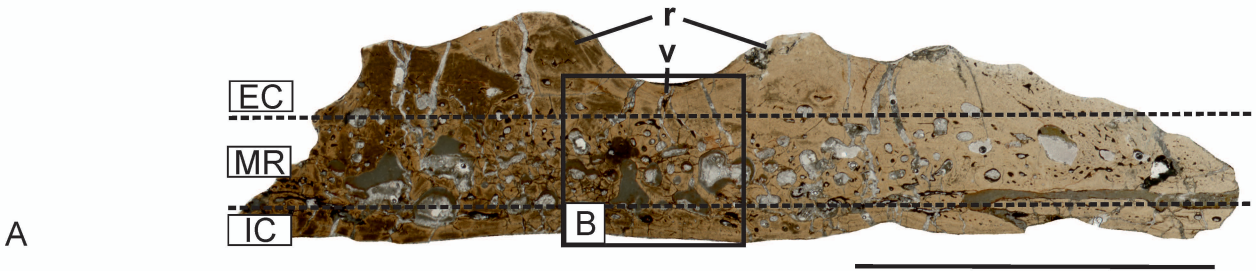
r
v
EC
MR
IC
B
A

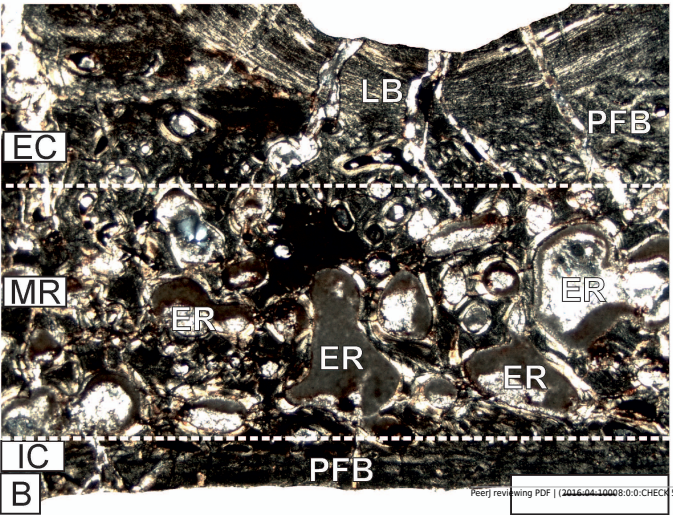
LB
PFB
EC
MR
ER
ER
ER
ER
IC
PFB
B

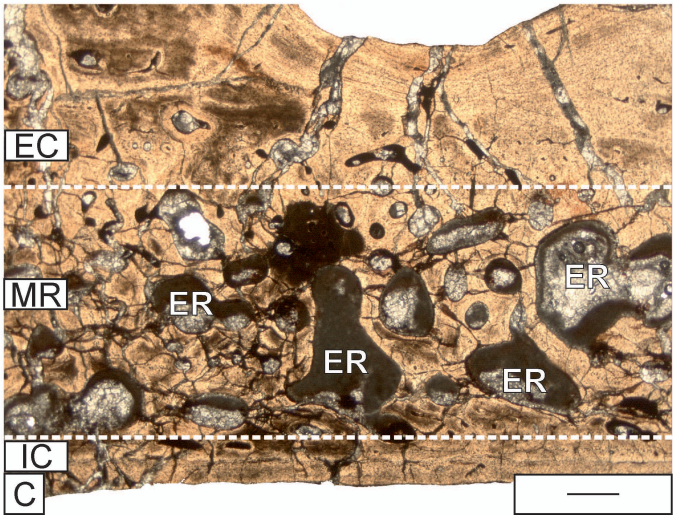
EC
MR
ER
ER
ER
ER
IC
C

Figure 5(on next page)

Histology of the external cortex of the skull bones of Metoposaurus krasiejowensis [i](UOPB 01029) from Late Triassic of Poland.

(A) **Fragment of external cortex of the frontal, image in plane-polarized light; (B)** Same as (A), but in cross-polarized light; (C) **External cortex of the tabular with distinct Sharpey's fibers in the area of the sculptural ridges, image in cross-polarized light; (D)** The resting lines (black arrows) in the cortex of squamosum2, image in plane-polarized light; (E) **The resting lines expressed as an alternation of lamellar layers and layers with distinct Interwoven Structural Fibers (ISF) in the external cortex of the postparietal, image in cross-polarized light; (F)** Zones and annuli present in the external cortex of the quadratojugal, image in cross-polarized light; (G) **Alternation of valleys and ridges in the postfrontal, image in cross-polarized light; note that remains of lamellar bone in the deep part of cortex are present, representing the bottom of a valley from an older generation. (H)** The cementing lines (black arrows) visible in the superficial part of the external cortex of the supratemporal. Dashed lines mark the approximate border between the external cortex/middle region/internal cortex. Scale bars equal for (A-E) and (H) 100 µm and for (F)-(G) 500 µm. Abbreviations: OL = osteocyte lacunae, FLB = fibro-lamellar bone, PO = primary osteons, SF = Sharpey's fibers, LB = lamellar bone, ISF = Interwoven Structural Fibers, A = annulus, Z = zone, r = ridge, v = valley.

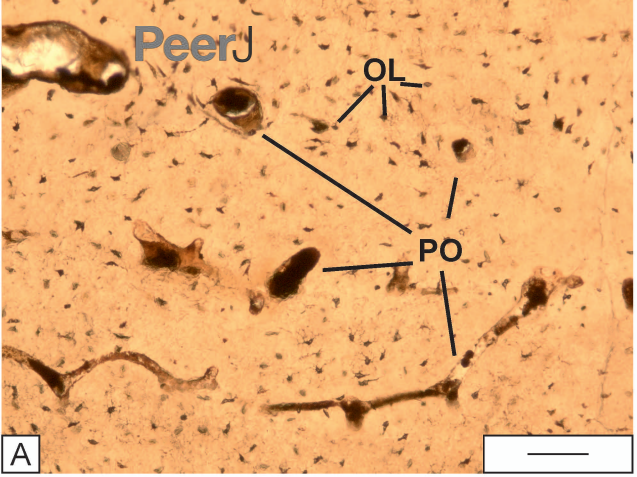

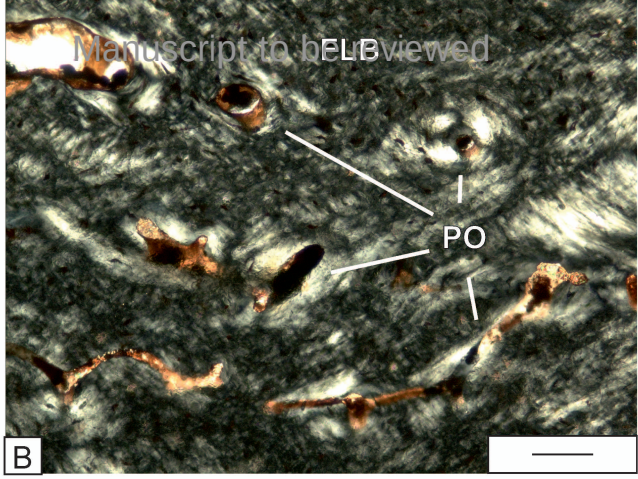

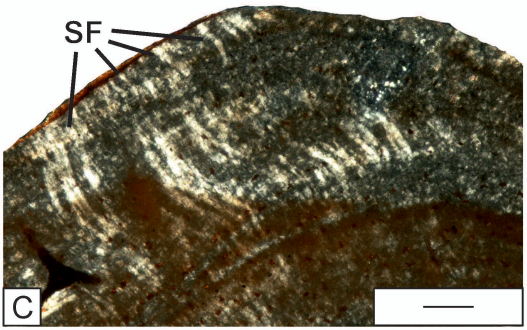

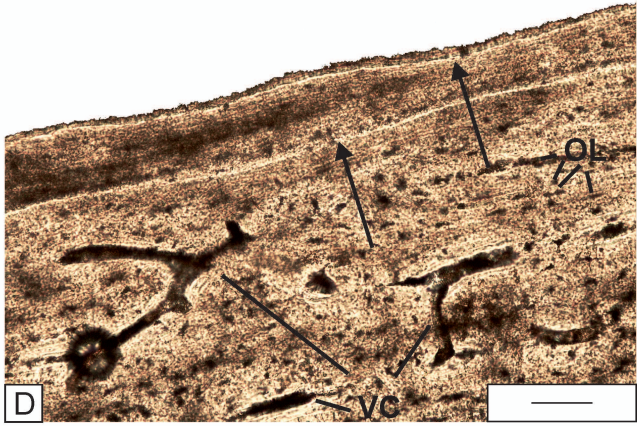

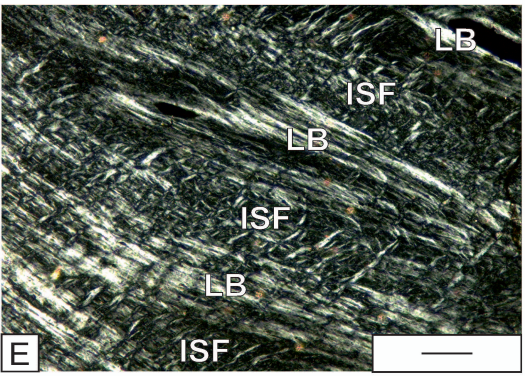

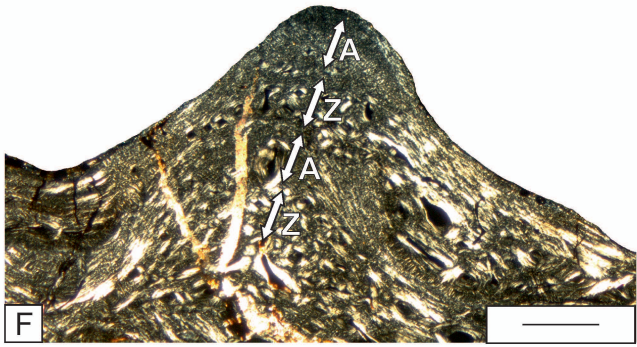

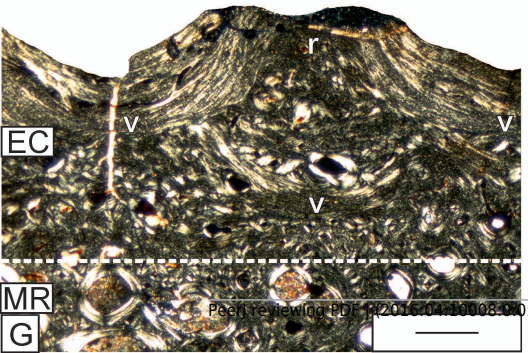

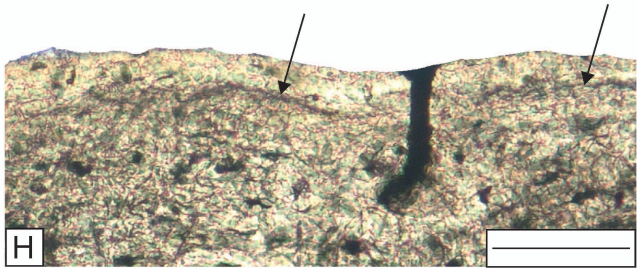

Figure 6(on next page)

The details of the histology of the middle region and internal cortex of the skull (UOPB 01029) bones of Metoposaurus krasiejowensis[i] from Late Triassic of Poland.

(A) **Large erosion cavities present in the middle region of the vomer; image in plane-polarized light; (B)** Poorly remodeled, well vascularized middle region of the parietal; image in plane-polarized light; (C) **Poorly vascularized fragment of the middle region of the squamosum2; image in plane-polarized light; (D)** Avascular internal cortex with resting lines (black arrows) visible in the parietal; image in plane-polarized light; (E) **Moderately vascularized internal cortex of the premaxilla; image in plane-polarized light; (F)** Highly vascularized internal cortex of the jugal; image in plane-polarized light; (G)[b] Alternation of thick annuli and zones visible in the internal cortex of the parasphenoid; image in cross-polarized light. Dashed lines mark the approximately border between the external cortex/middle region/internal cortex. Scale bars equal 100 µm for (D) and (G) and 500 µm for other photographs. Abbreviations: IC = internal cortex, MR = middle region, EC = external cortex, VC = vascular canals, A = annulus, Z = zone.

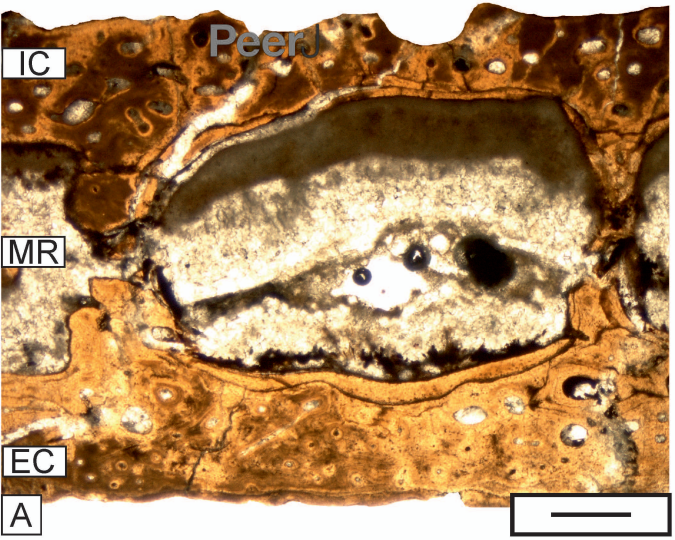

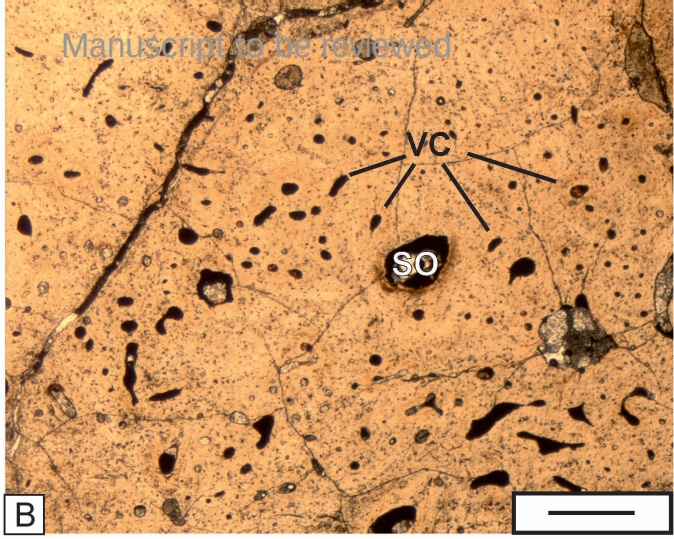

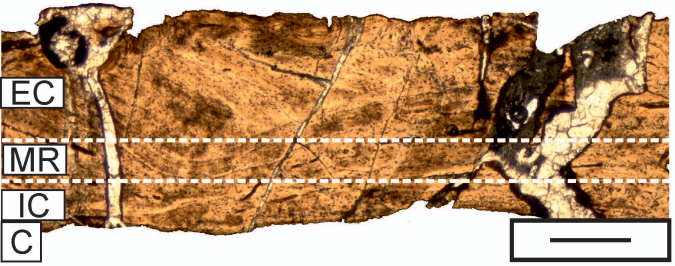

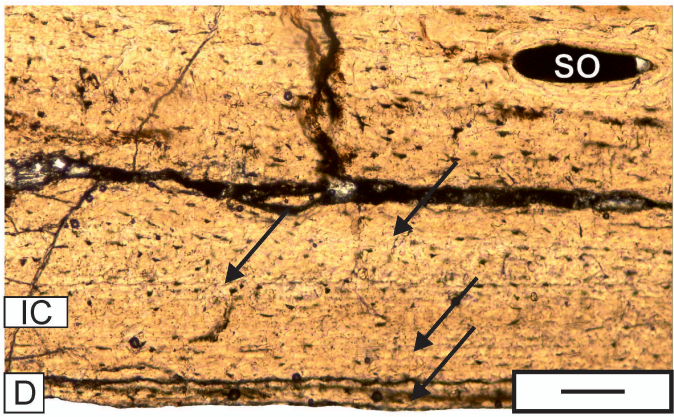

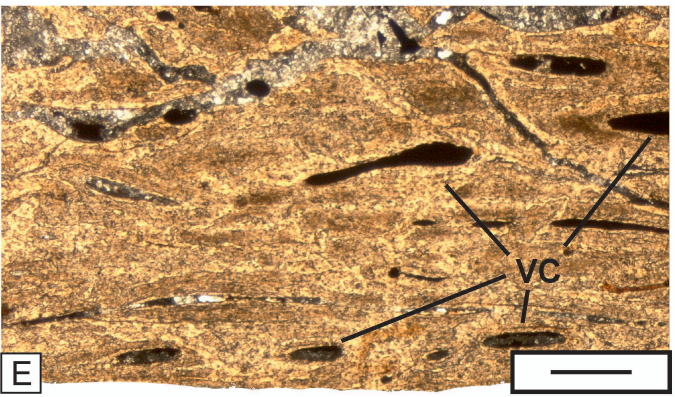

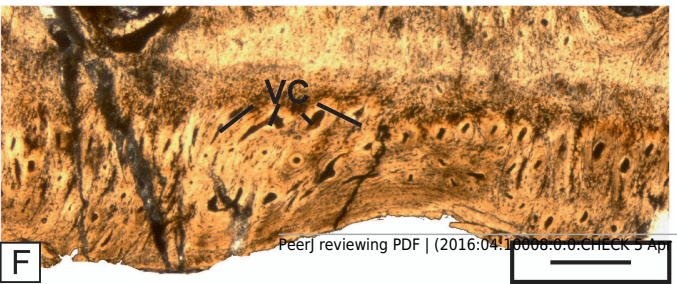

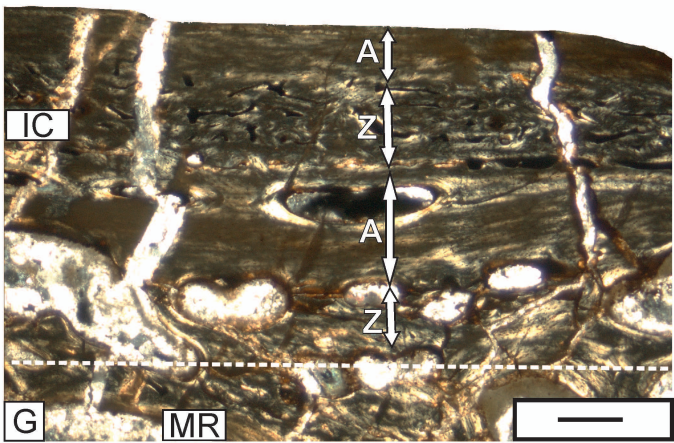

Figure 7 (on next page)

Histological details of the quadratum (A-C) and exooccipitale (D-H) of Metoposaurus krasiejowensis [i]skull (UOPB 01029) from Late Triassic of Poland.

(A) **Fragment of cortex of the quadratum; image in plane-polarized light; (B)** The same as (A), but in cross-polarized light; (C) **Trabecular bone of the quadrate bone; image in plane-polarized; (D)** Fragment of cortex of the exooccipitale with distinct Sharpey's fibers; image in cross-polarized light; (E) **Close-up of (D), note that the Sharpey's fibers are also visible in plane-polarized light; (F)** The same as (E) but in cross-polarized light; (G) **Trabeculae visible in the central part of the exooccipitale, image in plane-polarized light; (H)** Remains of calcified cartilage preserved in the trabeculae part of exoccipital, image in cross-polarized light. Scale bars equal 500 µm for (C), (D) and (G), and 100 µm for other photographs. Abbreviations: C = cortex, TR= trabecular region, OL = osteocyte lacunae, PO = primary osteons, PFL = parallel-fibred bone, VC = vascular canals, ER = erosion cavities, SO = secondary osteons, SF = Sharpey's fibers, CC = calcified cartilage.